

Synthesis and Optically Acid-Sensory and Electrochemical Properties of Novel Polyoxadiazole Derivatives

Tzi-Yi Wu, Rong-Bin Sheu, and Yun Chen*

National Cheng Kung University, Department of Chemical Engineering, No.1, Ta-Hsueh Road, Tainan, Taiwan 701, R.O.C.

Received October 17, 2003; Revised Manuscript Received November 21, 2003

ABSTRACT: A series of PPV-based polyoxadiazoles have been synthesized by Horner and Suzuki coupling polymerization to investigate their structure–property relationship. These copolymers exhibit good thermal stability (decomposition temperature around 352–413 °C). Excimer formation in **P4**–**P9** was confirmed by their absorption and PL spectral peak transition in solution at different concentrations and in thin films. Unusual absorption and fluorescence were observed in acid media and have been related to photoinduced charge transfer in alternating donor–acceptor architecture. The photoinduced charge transfer led to a blue shift in iminodibenzyl-containing copolymers (**P1**–**P3**) and a red shift in fluorene-containing copolymers (**P9**), reflecting the fact that iminodibenzyl is a stronger electron-donating unit. The electrochemical properties of the copolymers were evaluated by cyclic voltammetry and their highest occupied molecular orbital and the lowest unoccupied molecular orbit energy levels were estimated. The optical band gaps of the dioxadiazole-containing copolymers show great discrepancy with the electrochemical band gap energy due to the donor–acceptor feature of the dioxadiazole unit.

Introduction

Molecular sensory materials have recently attracted considerable attention due to their potential applications in the field of chemistry and biology.¹ The research of conjugated polymer-based fluorescent chemosensors is emerging as an area of current interest in these years.² The extended π -conjugation provides conjugated polymer-based chemical sensors with the signal amplification characteristics, which is their major merit over sensors based on small molecules.³

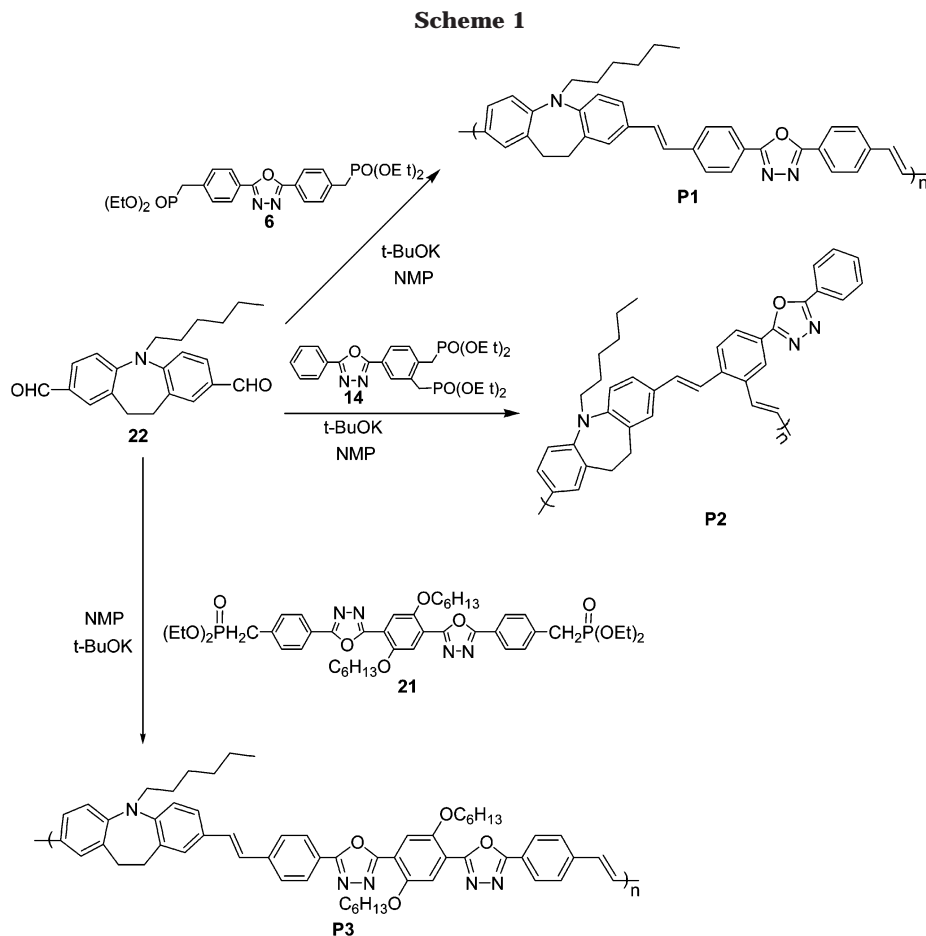
Almost all chemosensors based on conjugated polymers have been designed to have electron-donating groups such as crown ethers, aza crown ethers, calixarenes, and nitrogen-containing heterocycles for recognition of cation analytes such as proton and metal ions.¹ Moreover, many conjugated polymers having imine-type (C=N) nitrogen atom(s) in a heterocycle unit, such as pyridine,⁴ quinoline,⁵ benzoxazolyl,⁶ benzimidazolyl,⁷ and bipyridyl⁸ have been reported to exhibit colorimetric and fluorescent acid-sensory properties. A 1,3,4-oxadiazole ring can be thought to be a basic heterocycle due to the presence of imine-type nitrogen atoms with its lone pair electrons not participating in the aromatic sextet. Trifonov et al. reported the physicochemical and photophysical properties of 2,5-diphenyl-1,3,4-oxadiazole (**1a**) in acidic media.⁹ Protonation on the oxygen atom was unlikely because the corresponding cation form was very unstable. Moreover, protonation led to only one form of conjugate acid (**1b**), although **1a** had two equal basic centers. Huang et al. reported the spectroscopic properties of oxadiazole-containing conjugated polymers in solvent mixtures of chloroform (solvent for the polymer) and methanol (nonsolvent for the polymer) and found an unusual solvatochromism either in absorption or in emission.¹⁰ However, to our knowledge, there has been no report about the influence of an acid upon the optical properties of both iminodibenzyl-containing and oxadiazole-containing polymers.

Recently, we reported the synthesis and characterization of a series of luminescent copolymers with hole transport (carbazole, iminodibenzyl, phenothiazine, distyrylbenzene) and electron transport units (aromatic 1,3,4-oxadiazole).^{11–14} The advantageous physical properties of oxadiazole-containing polymeric materials, coupled with their interesting photophysical features, have prompted studies concerned with the nature of their excited state. These planar polymeric materials have been shown to have closely packed π -conjugated structures capable of interchain excimer as well as charge-transfer complex (exciplex) formation.¹⁵ In this study, we synthesized π -conjugated copolymers bearing hole-facilitating iminodibenzyl and distyrylbenzene moieties (donor) and electron-facilitating oxadiazole moieties (acceptor) in the main chain. Polymers possessing oxadiazole units are readily dissolved in strong acids, which induces protonation of the nitrogens in the oxadiazole units. Moreover, fluorene-based polyoxadiazole derivative, which bears no hole-facilitating moiety, is also prepared for comparison.

Results and Discussion

Synthesis and Characterization of Polymers. Synthetic routes of copolymers **P1**–**P8** using the Horner–Wadsworth–Emmons reaction are shown in Schemes 1–3. Structurally, **P1**–**P8** all consist of alternate donor and acceptor segments in the main chain or as side groups. For example, **P1**–**P3** consist of alternate iminodibenzyl (electron-donating) and aromatic 1,3,4-oxadiazole (electron-accepting) in the main chain. However, the donor segment of **P4**–**P6** is 2,5-bis(dodecyloxy)-distyrylbenzene chromophores instead. The electrophilic aromatic 1,3,4-oxadiazole chromophores in **P4**, **P5**, and **P6** are identical to those of **P1**, **P2**, and **P3**, respectively. But in **P2** and **P5**, the aromatic 1,3,4-oxadiazole chromophores are attached as side groups. Moreover, **P3** and **P6** possess aromatic dioxadiazoles in the backbones and extra hexyloxy groups in the side chains. In the main

* Corresponding author. E-mail: yunchen@mail.ncku.edu.tw.



chain, **P7** consists of alternate bis(hexyloxy)benzene and aromatic dioxadiazole, whereas in **P8** the donor and acceptor are hexaalkoxytris(phenylenevinylene) and aromatic oxadiazole, respectively. **P1** and **P4** exhibited poor solubility in chloroform and tetrahydrofuran (THF) due to the rigid rod structure of the oxadiazole unit. Regardless of attached hexyloxy groups in the side chain, **P6** was still insoluble in tetrahydrofuran due to an extra oxadiazole in the backbone. However, when the aromatic 1,3,4-oxadiazole chromophores were attached as side groups, such as in **P2** and **P5**, the solubility in chloroform and tetrahydrofuran was greatly enhanced. Moreover, **P3** and **P7** exhibited good solubility in chloroform and tetrahydrofuran.

The dioxadiazole dibromide (**29**) was synthesized from hydrazine dichloride (**17**) and 4-bromobenzoyl chloride (**27**), followed with a ring-closing reaction in POCl_3 (Scheme 4). Then we prepared **P9** composed of fluorene and dioxadiazole units using palladium-catalyzed Suzuki coupling reactions between fluorene diboronate **30** and the dioxadiazole dibromide **29** in toluene. **P9** was obtained as a pale yellow powder in a high yield of 91%. **P9** was completely soluble in common organic solvents, such as chloroform and tetrahydrofuran, probably contributed by the soft hexyl and hexyloxy side chains attached to the fluorene moiety and the dioxadiazole unit, respectively.

The molecular weights of these copolymers were determined by gel permeation chromatography using monodisperse polystyrenes as the standard. As depicted in Table 1, the weight-average molecular weights (M_w) are between 9500 and 17 600 with polydispersity indices (M_w/M_n) in the range 1.27–1.92. However, those of **P1**,

Table 1. Properties of the Polymers

	yield	η_{red} (dL/g) ^a	M_n^b	M_w^b	PDI ^b	T_g (°C)	T_d^c (°C)
P1 ^d	55	0.28				202	390
P2	54	0.21	7460	9490	1.27		385
P3	61	0.19	7120	9750	1.37		357
P4 ^d	53	0.20				197	387
P5	58	0.26	11000	15000	1.36		376
P6 ^d	91	0.17					413
P7	89	0.29	13700	17600	1.29		390
P8	86	0.17	6100	10050	1.65		352
P9	91	0.29	7350	14100	1.92	152	412

^a Reduced viscosity: measured at 30 °C with a concentration of 0.15 g/dL in NMP (**P1–P5**), 1,1,2,2-tetrachloroethane (**P6**), and chloroform (**P7–P9**). ^b M_n , M_w , and PDI of the polymers were determined by gel permeation chromatography using polystyrene standards in THF. ^c The temperatures at 5% weight loss. ^d **P1**, **P4**, and **P6** were partially soluble or insoluble in THF.

P4, and **P6** could not be obtained due to their limited solubility in THF. The reduced viscosities (η_{red}) of these copolymers are in the range 0.17–0.29 dL/g. Thermal behaviors were evaluated by means of differential scanning calorimetry (DSC) and thermogravimetric analysis (TGA), and the decomposition temperatures of **P1–P9** were about 352–413 °C, as determined at 5 wt % loss. The glass transition temperature (T_g) of **P1**, **P4**, and **P9** were determined to be 202, 197, and 152 °C, whereas the other copolymers are basically amorphous materials because no phase transitions could be observed up to 300 °C in their DSC thermograms.

Optical Properties. The optical characteristics of these copolymers were investigated both in solution and in the film state. Their absorption and emission spectral data are summarized in Table 2. The optical and

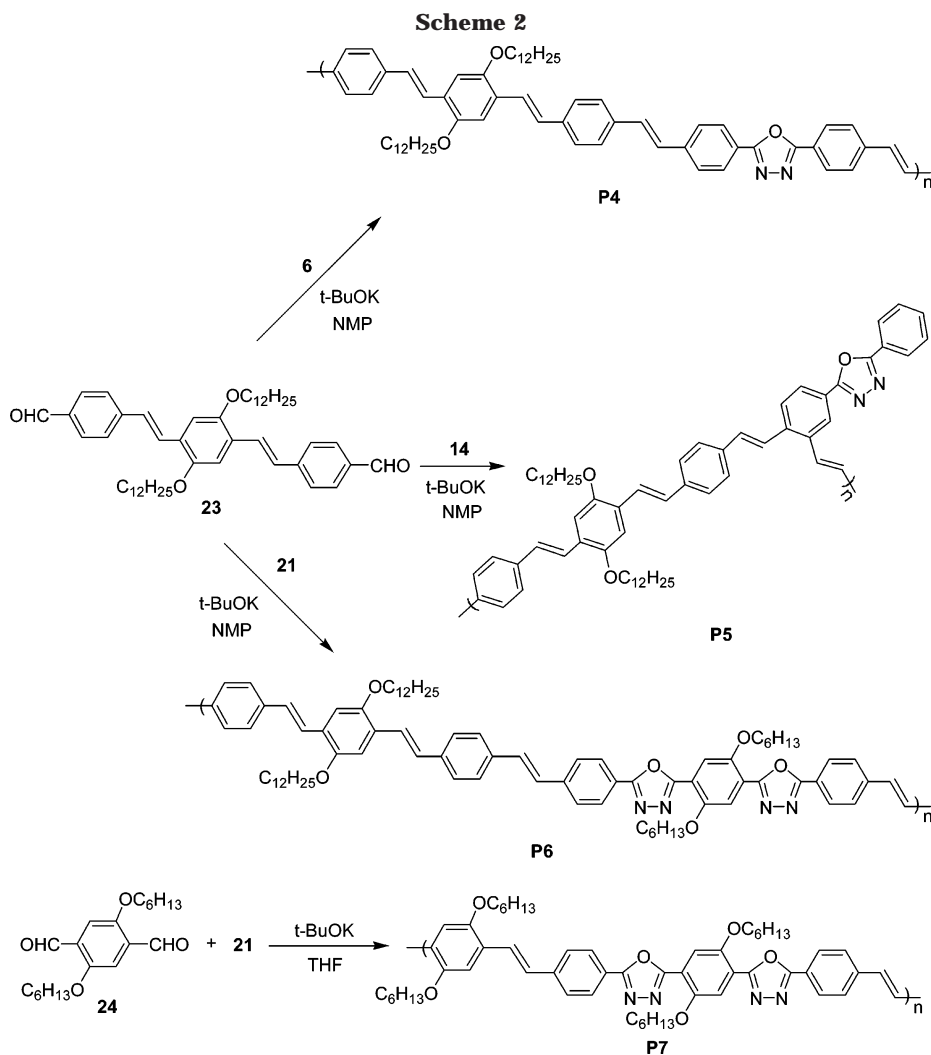


Table 2. Optical Properties of Polymers P1–P9 in Film and Solution States at Room Temperature

	UV _{solution} (nm)	UV _{film} (nm)	PL _{solution} (nm)	PL _{film} (nm)	Stokes shift ^a (nm)
P1^b	328, 402	408	511	520	112
P2	307, 370	310, 372	504	509	137
P3	331, 403	334, 417	508	513	96
P4^b	362, 442	382, 459	515, 547	550	91
P5	359, 433	359, 445	515, 547	549	104
P6^b	445	462	525	544	82
P7	353, 422	331, 440	492, 517	517, 540	100
P8	348, 465	493	548	586	93
P9	362, 386	366, 394	419, 438	431, 450	56

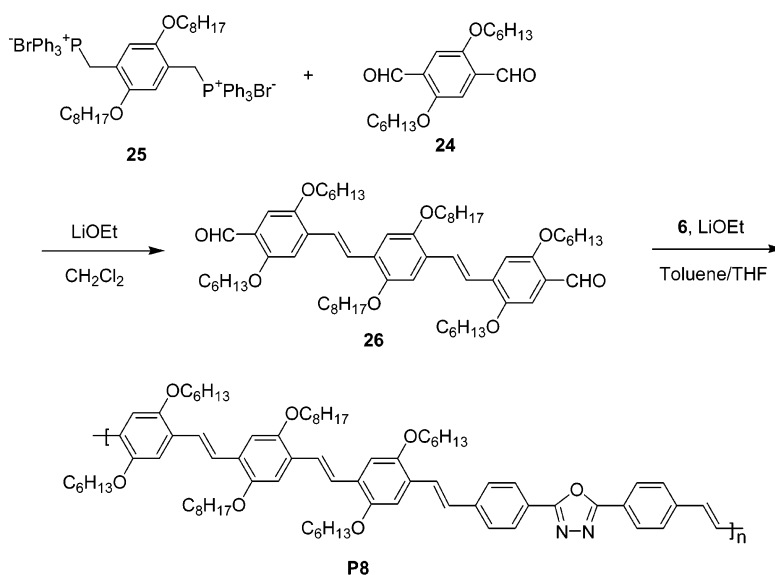
^a Stokes shift = PL_{film}/nm – UV_{film}/nm. ^b UV–visible absorption and photoluminescence spectra of polymers in C₂H₂Cl₄ solution.

electrochemical properties of **P1–P9** can be categorized according to the types of the donor and acceptor segments to elucidate the structure–property relationship. Copolymers **P1–P3** consist of alternate electron-donating iminodibenzyl and electron-accepting aromatic 1,3,4-oxadiazole chromophores. The structure of **P2** is similar to that of **P1** except that the aromatic 1,3,4-oxadiazole chromophores are attached as side groups. Compared structurally with **P1**, **P3** possesses an extra oxadiazole in the backbone and hexyloxy group in side chain. In the film state, **P1** shows one major absorption maximum (λ_{\max}) at about 408 nm (Figure 2a in the Supporting Information), whereas **P2** exhibits two blue-shifted absorption bands at about 310 and 372 nm. This suggests that the pendant structure in **P2** does exert a

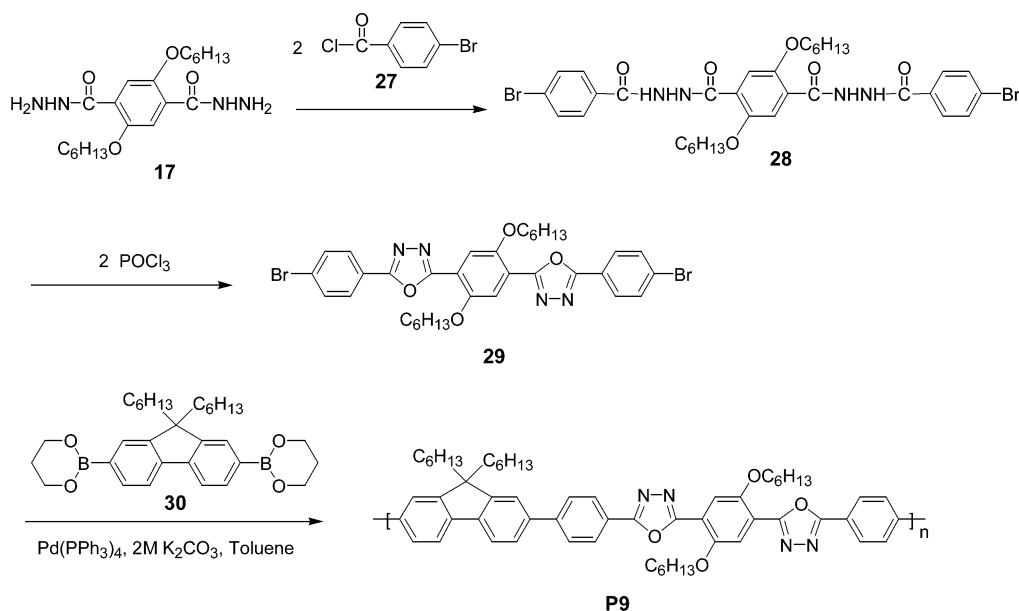
significant effect on its electronic band structure. The two absorption maxima of **P2** in the film state can be ascribed to the $n-\pi^*$ transition of pendant 1,3,4-oxadiazole segments (310 nm) and the $\pi-\pi^*$ transition of iminodibenzyl chromophores conjugated with pendant 1,3,4-oxadiazole segments (372 nm). Compared with **P1**, aromatic dioxadiazole segments in **P3** brings about a red shift in the absorption maxima and a blue shift in the PL maxima. These characteristics may bring about a great discrepancy between electrochemically and optically estimated band gap energies. However, replacing the oxadiazole moiety in **P1** with a pendant oxadiazole (in **P2**) results in a blue shift of both absorption and PL, implying decreased effective conjugation in the polymer main chain. The order of the Stokes shifts is **P2** > **P1** > **P3**. A high Stokes shift in **P2** suggests its greater energy dissipation during the lifetime of the excited state before return to the ground state.

The structures of **P4**, **P5**, and **P6** are similar to those of **P1**, **P2**, and **P3**, respectively, except that the distyrylbenzene chromophore is incorporated instead of iminodibenzyl group. Compared with **P4** (Figure 2b in the Supporting Information), extended aromatic dioxadiazole chromophores in **P6** also bring about a slight red shift in the absorption maxima and a blue shift in PL maxima. However, **P4** exhibits two PL maxima (515 and 547 nm) in solution (10^{-5} M in C₂H₂Cl₄, Figure 6 in the Supporting Information) and one maximum (550 nm) in the film state. The peak located in the longer

Scheme 3



Scheme 4



wavelength region can be explained in terms of aggregation and fluorescence excimer formation.^{17–21}

The copolymers **P1**, **P4**, and **P8** comprise of alternate electron-accepting aromatic 1,3,4-oxadiazole chromophores and electron-donating moieties in the backbone. The electron-donating moieties of **P1** and **P4** are iminodibenzyl and 2,5-bis(dodecyloxy)-1,4-distyrylbenzene, respectively. Compared structurally with **P4**, **P8** possesses four extra hexyloxy groups attached at phenylene moieties as pendant groups. As shown in Supporting Information Figure 2c, **P4** exhibits greater absorption and PL bathochromic shifts (51 and 30 nm, respectively) than **P1**, presumably due to more extended conjugation in distyrylbenzene chromophores conjugated with oxadiazole groups or aggregation and fluorescence excimer formation. In film states, **P8** exhibits a 34 nm red shift in absorption and a 36 nm red shift in PL as compared with those of **P4**, implies the electron-releasing effect of six alkoxy chains.

The copolymers **P3**, **P6**, **P7**, and **P9** are composed of alternate aromatic dioxadiazole and various electron-donating moieties in the main chain. For example, the

electron-donating moieties of **P3** and **P6** are iminodibenzyl and 2,5-bis(dodecyloxy)-1,4-distyrylbenzene, respectively. The structure of **P7** (or **P9**) is similar to those of **P6**, except that the bis(hexyloxy)benzene (or fluorene) is incorporated instead. As shown in Supporting Information Figure 2d, the absorption spectrum of **P6** is red-shifted in comparison with that of **P7**, which can be attributed to extended effective conjugation in **P6** relative to **P7**. **P9** exhibits two main emission peaks at 450 and 431 nm, corresponding to a blue emission. The presence of vibronic structures in its emission spectrum indicates that **P9** has a rigid and well-defined backbone structure.²²

Iminodibenzyl-containing copolymers (**P1–P3**) show similar PL spectra under different concentration (Figure 3 in Supporting Information) and the red shift in the film state can be attributed to aggregation formation. Figure 1 shows PL spectra of **P6–P9** in solution at different concentrations. In dilute solution, the PL spectra of **P6** are similar and exhibit a PL maximum at 515 nm with a shoulder at about 544 nm. The PL intensity first rises rapidly as the concentration in-

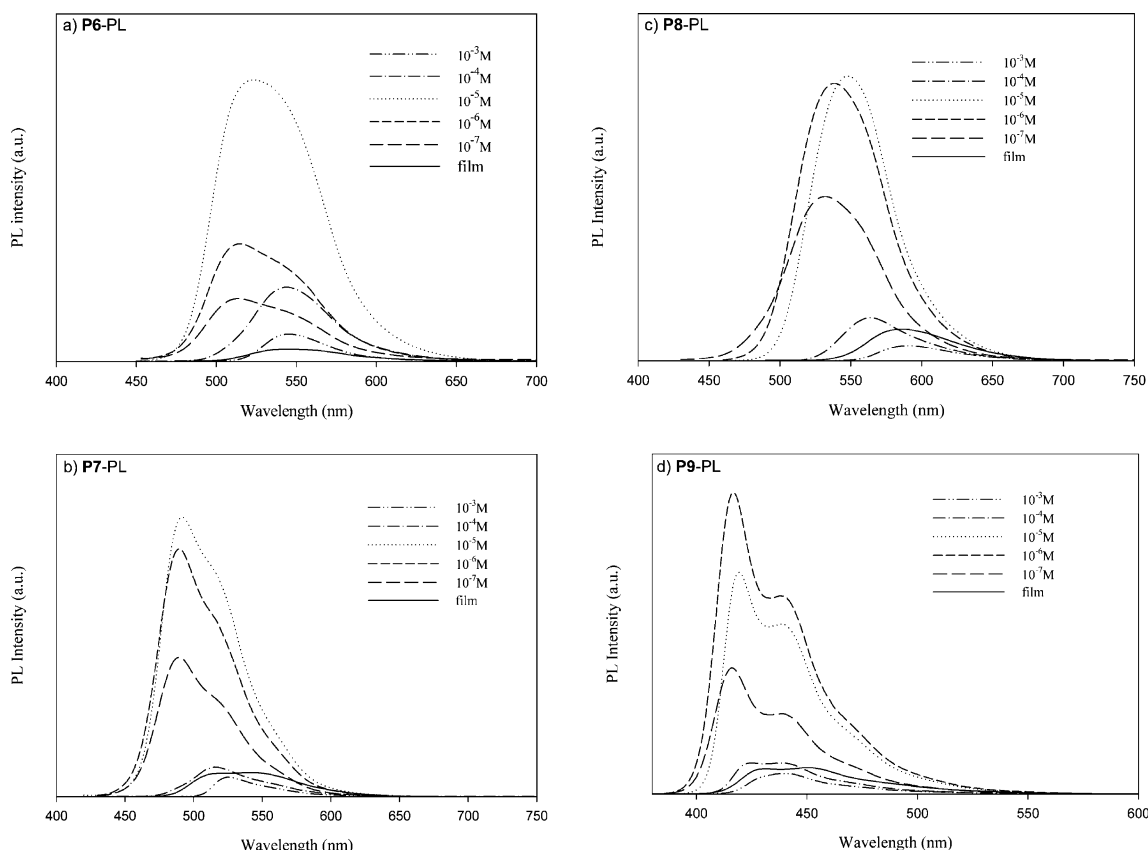


Figure 1. Photoluminescence spectra of **P6** in $C_2H_2Cl_4$, **P7**, **P8**, and **P9** in $CHCl_3$ at different concentrations. Excitation wavelength: 380 nm.

creases from 10^{-7} to 10^{-5} M, followed with a quick decrease at concentrations greater than 10^{-5} M. This could be attributed to the enhanced concentration quenching effect at higher concentration. Moreover, when the concentrations increase from 10^{-7} to 10^{-3} M, the PL maximum shifts to 544 nm and the emission at 515 nm disappears completely. In the condensed film state, the PL spectrum is similar to that in 10^{-3} M solution with lessened intensity. The PL spectra of **P6** in the solvent mixture of $C_2H_2Cl_4$ and CH_3OH exhibit a gradual peak transition ($522 \rightarrow 544$ nm) with an increasing ratio of CH_3OH (poor solvent) (Figure 4 in Supporting Information). However, the absorption spectra of **P6** are independent of concentration and polarity in the solution (Figure 5 in Supporting Information). Moreover, **P7–P9** exhibit similar PL spectra below 10^{-5} M with abrupt quench and bathochromic transition at concentrations greater than 10^{-5} M (Figure 1). The observation indicates that a new emitting species is formed in the concentrated solution and film state. We presume this red shift of emission bands in **P4–P9** is attributable to an excimer emission.²³ The excimer formation usually results in a longer wavelength and featureless emission that depends on the distance between the luminophores.

Optically Acid-Sensory Properties. The nitrogen in the 1,3,4-oxadiazole imine-type ring and iminodibenzyl chromophore have lone pair electrons not participating in the aromatic sextet. Protonation of these nitrogen atoms is likely to occur in acid media. Figure 2 shows the absorption and PL spectra of oxadiazole-containing (**3**, **19**) and iminodibenzyl-containing compound [*n*-hexyliminodibenzyl (**31**) and **P10**] in $CHCl_3$ and formic acid solutions. **31** and **P10**²⁴ were introduced to confirm the optically acid-sensory property of iminodibenzyl-

containing compounds. Oxadiazole-containing **3** and **19** show conspicuous absorption and PL spectral red shift in formic acid as compared to those in chloroform, implying the protonation of the lone pair in imine-type nitrogen atoms. On the contrary, iminodibenzyl-containing **31** and **P10** exhibit significant absorption and PL blue shift in formic acid. The blue shift would be attributable to the following reasons: (1) The nitrogen exerts an auxochromic effect on the iminodibenzyl chromophore via interaction between its lone pair electrons and the π -electrons, which apparently stabilized the π^* state and leads to a bathochromic shift by lowering its energy. These nonbonding electrons are readily protonated in acid media that leads to disappearance of the auxochromic effect and results in a hypsochromic shift.²⁵ (2) The coordination of acid brings about a deconjugation effect on the polymer backbone.¹

P1–P3 are alternating donor–acceptor conjugated copolymers, in which the essential π -electronic structure in the ground and excited states are expected to depend on the polarity of the solvent. The absorption and PL spectra of **P1–P3** in formic acid and 1,1,2,2-tetrachloroethane solutions are shown in Figure 3. The absorption bands of **P1** and **P2** in formic acid diminish and blue shift significantly as compared to those in 1,1,2,2-tetrachloroethane, whereas that of **P3** in formic acid exhibits only reduced intensity in absorption bands without a blue shift. Moreover, the PL spectra of **P1–P3** also exhibit slight quenching and conspicuous blue shifts upon dissolving in formic acid. Gradual PL spectral variations of **P1–P3** in chloroform upon addition of trifluoroacetic acid (TFA) have been recorded to observe the transformation processes (Figure 4). In **P1** and **P2** solution (10^{-5} M), addition of TFA gives rise to significant quenching of the main PL peak at 510 nm

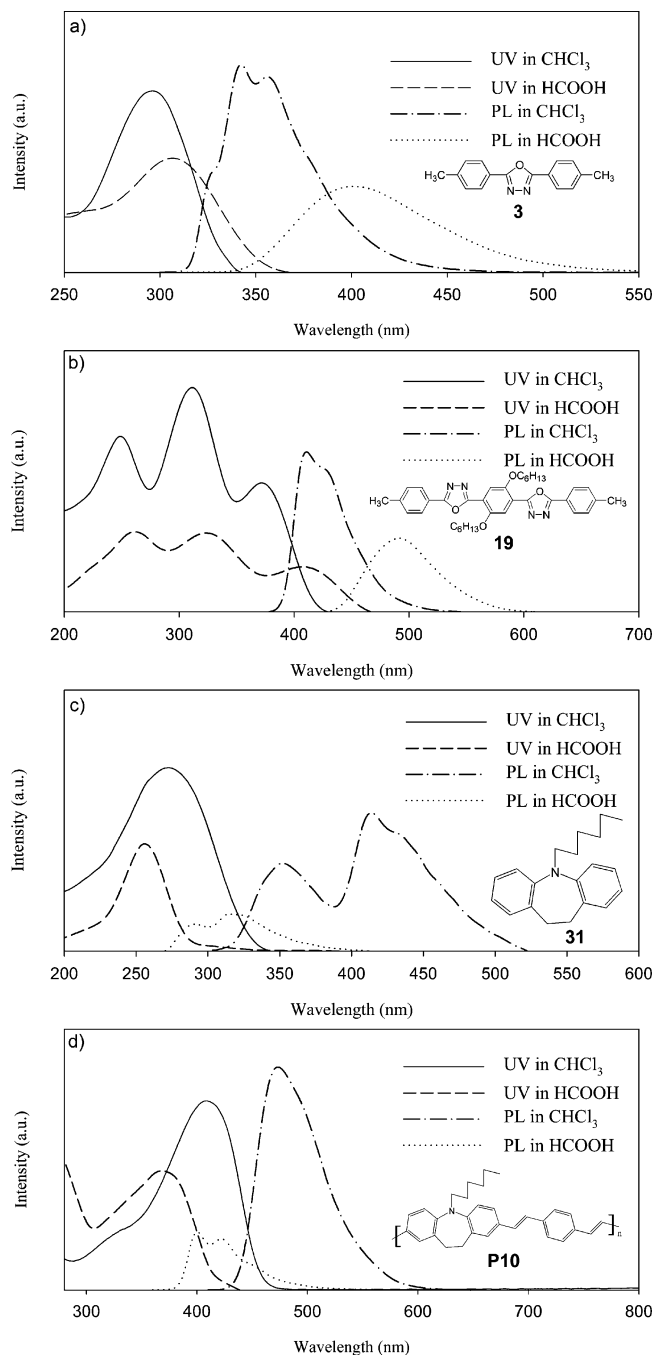


Figure 2. Absorption and photoluminescence spectra of **3**, **19**, *n*-hexyliminodibenzyl (**31**), and poly(*N*-hexyl-3,8-iminodibenzyl-1,2-ethynylene-1,4-phenylene-1,2-ethynylene) (**P10**) in CHCl_3 and HCOOH solutions.

below 3×10^{-3} M. The main peak disappears completely and two new peaks appear at shorter wavelength region (417 and 448 nm) when the TFA concentration exceeds 10^{-2} M. However, in **P3** the PL spectra show similar significant quenching in TFA solution, but with gradual blue shifts. The slight discrepancy between **P3** and **P1** can be attributed to the difference in effective conjugation lengths in oxadiazole chromophores. The fluorescence transformation of **P1–P3** in acidic media seems due to photoinduced charge transfer between iminodibenzyl and oxadiazole units.²⁶ The dipole moments of the donor–acceptor pairs are different in the excited state and ground state. When acid interacts with the iminodibenzyl group (donor), the excited state is more strongly destabilized by the acid than the ground state,

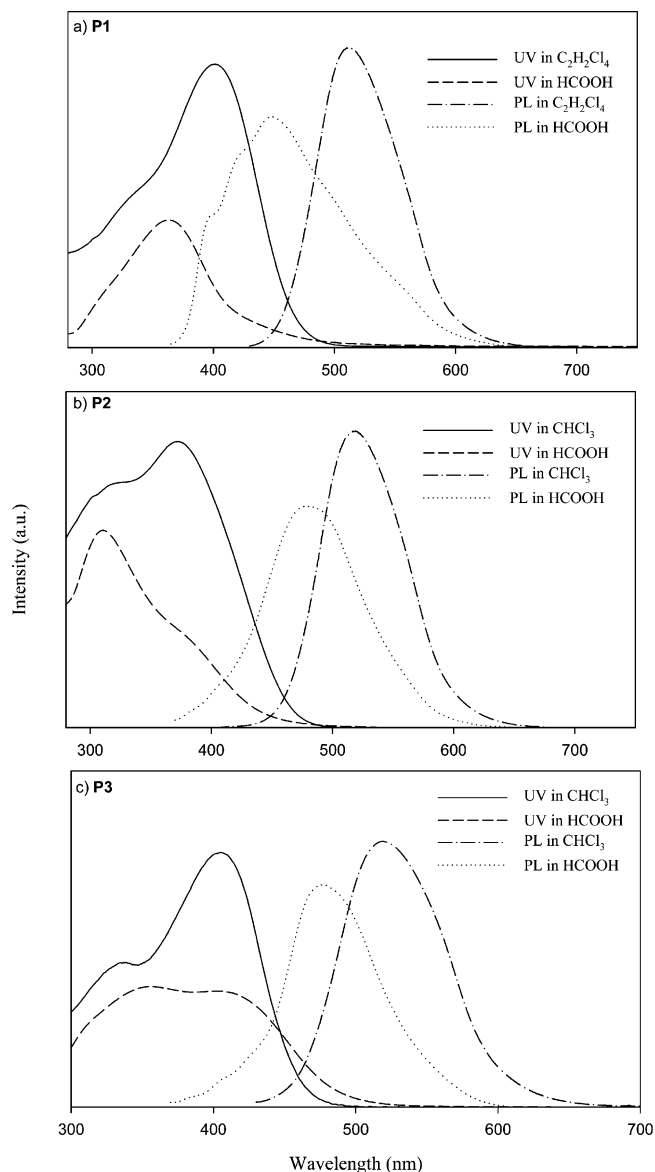


Figure 3. Absorption and photoluminescence spectra of **P1–P3** in HCOOH solution (10^{-6} M polymer solution).

and a blue shift of the absorption and emission spectra is expected (Figure 5a). Conversely, when acid interacts with the oxadiazole group (acceptor), the excited state is more stabilized by acid than the ground state, and this leads to a red shift of the absorption and emission spectra (Figure 5b). Therefore, in **P1–P3**, TFA protonates iminodibenzyl chromophores more likely than oxadiazole rings and leads to obvious blue shift in absorption and PL spectra.

Figure 6 shows the PL spectral variations of **P7** and **P9** in chloroform solution with various TFA concentrations. Upon adding TFA, **P7** exhibits significant quenching and the shoulder at 524 nm is red-shifted to 555 nm. Moreover, **P9** shows similar significant PL quench and gradual red shifts of shoulder from 438 to 500 nm. The phenomena are attributable to protonation of aromatic dioxadiazole chromophores in acidic media.

Electrochemical Properties. When materials are used as an emissive layer for organic light-emitting diodes (OLEDs) or as a donor (or acceptor) component in organic photovoltaic devices (OPVDs), matches of their valence band (HOMO) and conduction band (LUMO) energy levels with work functions of the

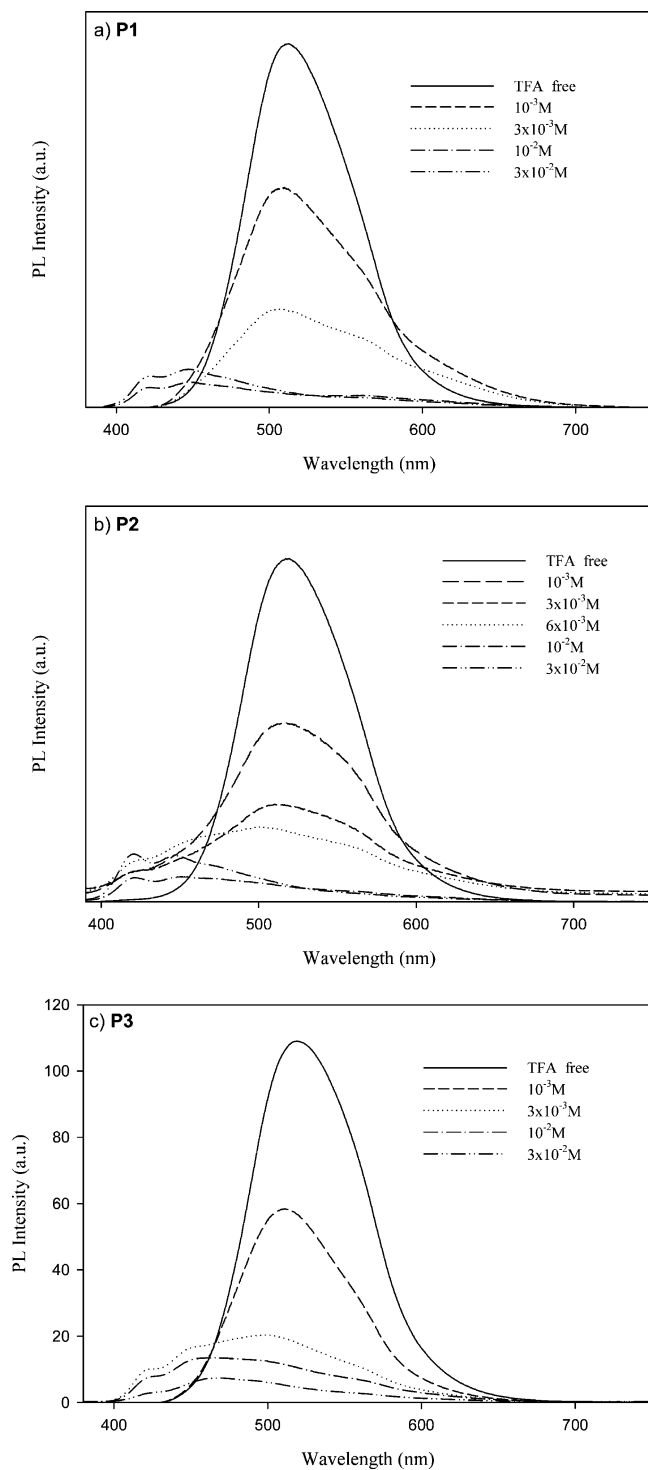


Figure 4. Photoluminescence spectra of **P1–P3** in chloroform (10^{-5} M) containing different concentrations of trifluoroacetic acid.

electrodes are of paramount importance. Table 3 summarizes the electrochemical properties of **P1–P9**, and Figure 7 shows the cyclic voltammograms of **P1–P9** in an anodic scan. Copolymers **P4** and **P6** comprise the same distyrylbenzene segment in the main chain, but **P6** possesses extra oxadiazole in the backbone and hexyloxy groups in side chain. The $E_{\text{onset(ox)}}$ of **P4** (0.8 V) is greater than **P6** (0.73 V), implying that the 1,4-bis(hexyloxy)benzene unit between two 1,3,4-oxadiazole rings reduces the $E_{\text{onset(ox)}}$ of **P6**. The $E_{\text{onset(ox)}}$ of **P8** (0.66 V) is the lowest among the copolymers investigated; it demonstrates that six electron-donating alkyloxy groups

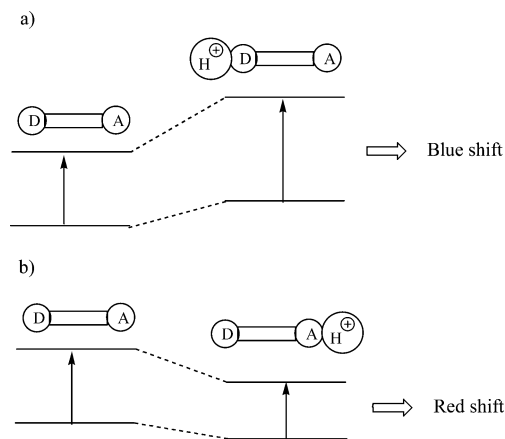


Figure 5. Schematic description of spectral displacements resulting from interaction of acid with an (a) electron-donating and (b) electron-withdrawing group.

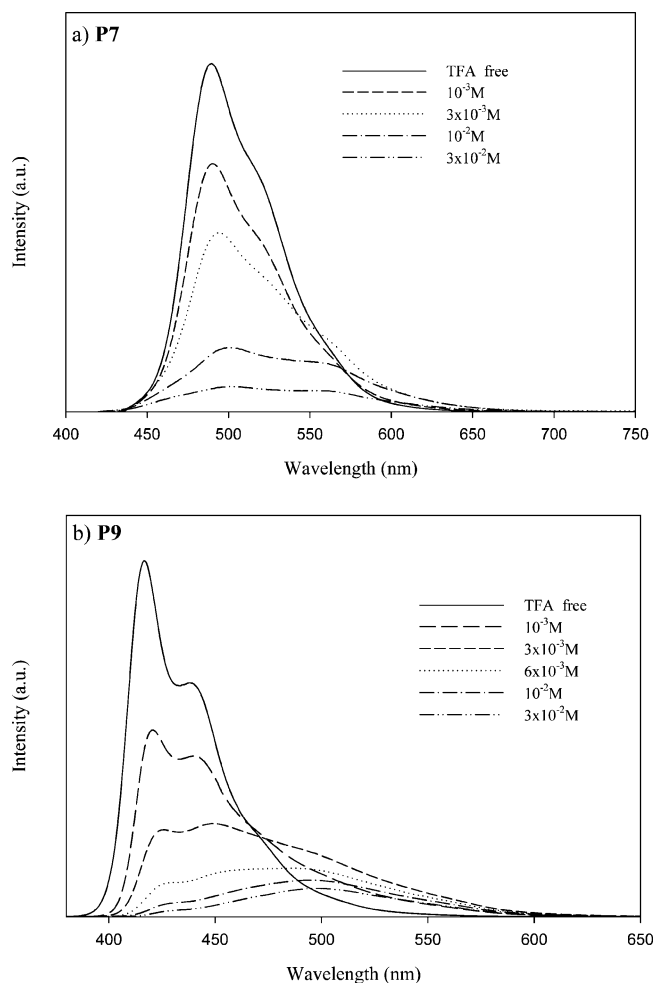


Figure 6. Photoluminescence spectra of **P7** and **P9** in trifluoroacetic acid/chloroform (10^{-6} M polymer solution).

dramatically decrease the oxidative onset potentials of the conjugated copolymers. The $E_{\text{onset(ox)}}$ of **P9** (1.23 V) is the largest and is 0.5 V greater than that of **P6** (0.73 V) having the distyrylbenzene segments, which would arise from enhanced electron affinity in **P9** containing fluorene chromophores. On the basis of enhanced onset oxidation potential, it is concluded that **P9** with fluorene chromophores in the backbone is the most electronegative one among these copolymers.

As shown in Table 3, **P1** and **P4** show reduction onset potentials [$E_{\text{onset(red)}}$] similar to those of **P2** and **P5**,

Table 3. Electrochemical Properties and Band Gap of Polymers P1–P9

	$E_{\text{onset(ox)}}$ VS Ag/AgCl(V)	$E_{\text{onset(ox)}}$ VS E_{FOC}^a (V)	$E_{\text{onset(red)}}$ VS E_{FOC}^a (V)	HOMO(IP ^d) (eV)	LUMO(EA ^e) (eV)	$E_{\text{g}}^{\text{elec } b}$ (eV)	$E_{\text{g}}^{\text{opt } c}$ (eV)
P1	0.84	0.38	-1.71	-5.18	-2.63	2.55	2.53
P2	0.90	0.44	-1.70	-5.24	-2.64	2.60	2.58
P3	0.85	0.38	-1.47	-5.18	-2.86	2.32	2.63
P4	0.80	0.34	-1.51	-5.14	-2.83	2.31	2.26
P5	0.81	0.35	-1.51	-5.15	-2.83	2.32	2.29
P6	0.73	0.26	-1.35	-5.06	-2.98	2.08	2.30
P7	0.88	0.41	-1.27	-5.21	-3.06	2.15	2.35
P8	0.66	0.19	-1.42	-4.99	-2.91	2.08	2.10
P9	1.23	0.76	-1.46	-5.56	-2.87	2.69	2.81

^a For **P1**, **P2**, **P4**, and **P5**, $E_{\text{FOC}} = 0.46$ V vs Ag/AgCl. For **P3**, **P6**, and **P7–P9**, $E_{\text{FOC}} = 0.47$ V vs Ag/AgCl. ^b Band gaps determined from the cyclic voltammogram. ^c Band gaps determined from the UV/vis absorption spectrum. ^d Ionization potential: $\text{IP} = E_{\text{onset(ox)}} - E_{\text{FOC}} + 4.8$. ^e Electron affinity: $\text{EA} = \text{IP} - E_{\text{g}}^{\text{opt}}$.

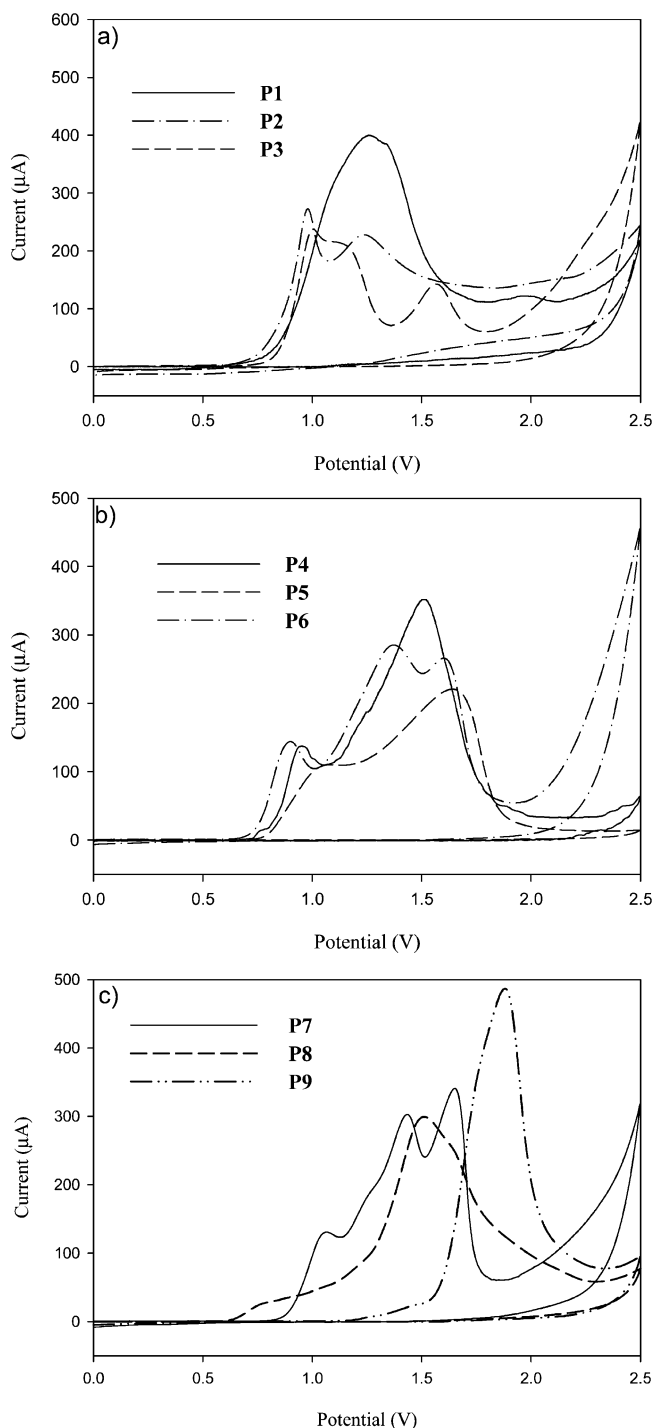


Figure 7. Cyclic voltammogram of **P1–P9** in 0.1 M *n*-Bu₄NClO₄/acetonitrile solvent with a scan rate of 100 mV/s.

respectively, suggesting that electron affinity of the 1,3,4-oxadiazole is not greatly affected whether it is incorporated in the backbone or as a pendant group. However, the copolymers containing dioxadiazole in the backbone, such as in **P3** and **P6**, the $E_{\text{onset(red)}}$ are more readily reduced due to promoted electron affinity. The electrochemically determined band gaps ($E_{\text{g}}^{\text{elec}}$) of **P1**, **P2**, **P4**, **P5**, and **P8** are approximately the same as the optically determined ones ($E_{\text{g}}^{\text{opt}}$) estimated from their onset absorption. However, a conspicuous discrepancy between $E_{\text{g}}^{\text{opt}}$ and $E_{\text{g}}^{\text{elec}}$ was observed in **P3**, **P6**, **P7**, and **P9**, which have an electron-donating unit (1,4-bis-(hexyloxy)benzene unit) between two 1,3,4-oxadiazole units. The donor and acceptor nature of these copolymers would explain the conspicuous discrepancy between $E_{\text{g}}^{\text{elec}}$ and $E_{\text{g}}^{\text{opt}}$. Similar differences between $E_{\text{g}}^{\text{opt}}$ and $E_{\text{g}}^{\text{elec}}$ were also found in donor–acceptor alkoxy-substituted aryleneethynylene/arylenevinylene conjugated polymers by Egbe et al.²⁷ Moreover, the lower $E_{\text{g}}^{\text{elec}}$ of **P6**, **P7**, and **P8**, as compared with those of other copolymers, can be attributed to greater donor–acceptor feature in polymer backbone.

Several ways to evaluate HOMO and LUMO energy levels from the onset potentials, $E_{\text{onset(ox)}}$ and $E_{\text{onset(red)}}$, have been proposed in the literature.^{28–30} They were estimated here on the basis of the reference energy level of ferrocene (4.8 eV below the vacuum level) according to the following equation: ($\text{HOMO} = E_{\text{onset(ox)}} + 4.8 - E_{\text{FOC}}$) and ($\text{LUMO} = \text{HOMO} - E_{\text{g}}^{\text{opt}}$), respectively.¹⁶ The LUMO energy levels of **P3** and **P6** relative to vacuum are estimated to be -2.86 and -2.98 eV, respectively. Apparently, the electron-accepting ability of **P3** and **P6** has been greatly enhanced by incorporating a dioxadiazole group into the polymer backbone. Moreover, **P7** exhibits a lower HOMO (-5.21 eV) and LUMO (-3.06 eV) level than **P6**, suggesting that the higher the weight ratio of dioxadiazole units, the lower the LUMO and HOMO levels. **P8** shows the highest HOMO level among the copolymers, probably due to its extended distyryl-benzene structure substituted with six electron-donating alkoxy groups. Moreover, the HOMO levels of **P1–P8** are between -4.99 and -5.24 eV, which may provide a closer match to the work function of ITO (-4.8 eV) when used as emitting materials in OLEDs and OPVDs.

Conclusion

We have synthesized a series of PPV-based polyoxadiazoles (**P1–P9**), which are thermally stable below 350 °C. The optical study demonstrates that the emission color of the resulting materials varies from blue to yellow and is dependent on the substituents (π -donor and π -acceptor groups) on both sides of the conjugated backbones. Compared with the absorption and PL

spectra of **P1**, **P3** with two oxadiazole rings per repeated unit brings about a red shift in absorption maxima and a blue shift in PL maxima. **P1–P3** display obvious blue shifts in trifluoroacetic acid/chloroform solutions. However, **P9** is bathochromic when protonated with trifluoroacetic acid in chloroform solutions. Electrochemical analysis through cyclic voltammetry demonstrates that these copolymers containing electron-accepting oxadiazole rings decrease the LUMO level significantly. The E_{onset} of **P9** with the fluorene rings in the backbone is higher than that of **P6** having the distyrylbenzene rings due to the increase of electron affinity after the fluorene ring is introduced into the polymer backbone. The electrochemical band gap calculated from the onset of the reduction and oxidation process show great discrepancy with the optical band gap calculated from the absorption edges due to donor–acceptor feature of the dioxadiazole unit.

Acknowledgment. We thank the National Science Council of the Republic of China for financial aid through project NSC 90-2216-E006-036.

Supporting Information Available: Experimental details and characterization of monomers (**6**, **14**, **21**, **26**, **29**) and copolymers (**P1–P9**), ^1H NMR spectrum (400 MHz, CDCl_3) of compound **26**, absorption and PL spectra of **P1–P9** in solution or film state, and reduction CV curves of **P1–P9**. This material is available free of charge via the Internet at <http://pubs.acs.org>.

References and Notes

- (1) McQuade, D. T.; Pullen, A. E.; Swager, T. M. *Chem. Rev.* **2000**, *100*, 2537.
- (2) Bobacka, J.; Ivaska, A.; Lewenstam, A. *Electroanalysis* **2003**, *15*, 366.
- (3) Swager, T. M. *Acc. Chem. Res.* **1998**, *31*, 201.
- (4) Yun, H.; Kwei, T. K.; Okamoto, Y. *Macromolecules* **1997**, *30*, 4633.
- (5) Jenekhe, S. A.; Lu, L.; Alam, M. M. *Macromolecules* **2001**, *34*, 7315.
- (6) So, Y. H.; Zaleski, J. M.; Murllick, C.; Ellaboudy, A. *Macromolecules* **1996**, *29*, 2783.
- (7) Yamamoto, T.; Sugiyama, K.; Kanbara, T.; Hayashi, H.; Etori, H. *Macromol. Chem. Phys.* **1998**, *199*, 1807.
- (8) Eichen, Y.; Nakhmanovich, G.; Gorlik, V.; Epshtein, O.; Poplawski, J. M.; Ehrenfreund, E. *J. Am. Chem. Soc.* **1998**, *120*, 10463.
- (9) Trifonov, R. E.; Ritschhev, N. I.; Ostrovskii, V. A. *Spectrochim. Acta A* **1996**, *52*, 1875.
- (10) Yu, W. L.; Meng, H.; Pei, J.; Huang, W.; Li, Y. F.; Heeger, A. J. *Macromolecules* **1998**, *31*, 4838.
- (11) Hwang, S. W.; Chen, Y. *Macromolecules* **2002**, *35*, 5438.
- (12) Chen, Y.; Huang, Y.-Y.; Wu, T.-Y. *J. Polym. Sci. Part A: Polym. Chem.* **2002**, *40*, 2927.
- (13) Hwang, S. W.; Chen, Y. *Macromolecules* **2001**, *34*, 2981.
- (14) Chen, Y.; Lai, S.-P. *J. Polym. Sci. Part A: Polym. Chem.* **2001**, *39*, 2571.
- (15) Jenekhe, S. A.; Osaheni, J. A. *Science* **1994**, *265*, 765.
- (16) Wu, T.-Y.; Chen, Y. *J. Polym. Sci. Part A: Polym. Chem.* **2002**, *40*, 3847.
- (17) Wu, T.-Y.; Chen, Y. *J. Polym. Sci. Part A: Polym. Chem.* **2002**, *40*, 4452.
- (18) Wu, T.-Y.; Chen, Y. *J. Polym. Sci. Part A: Polym. Chem.* **2002**, *40*, 4570.
- (19) Liu, B.; Yu, W. L.; Lai, Y. H.; Huang, W. *Chem. Mater.* **2001**, *13*, 1984.
- (20) Janietz, S.; Anlauf, S. *Macromol. Chem. Phys.* **2002**, *203*, 427.
- (21) Chang, R.; Hsu, J. H.; Fann, W. S.; Yu, J.; Lin, S. H.; Lee, Y. Z.; Chen, S. A. *Chem. Phys. Lett.* **2000**, *317*, 153.
- (22) Zheng, M.; Ding, L. M.; Lin, Z. Q.; Karasz, F. E. *Macromolecules* **2002**, *35*, 9939.
- (23) Sun, S. S.; Lee, A. J. *J. Photochem. Photobiol. A* **2001**, *140*, 157.
- (24) Chen, Y.; Wu, T.-Y. *Polymer* **2001**, *42*, 9895.
- (25) Skoog, D. A.; Holler, F. J.; Nieman, T. A. *Principles of Instrumental Analysis*, 5th ed.; Harcourt Brace & Co.: New York, 1998; Chapter 15.
- (26) Valeur, B.; Leray, I. *Coord. Chem. Rev.* **2000**, *205*, 3.
- (27) Egbe, D. A. M.; Cornelia, B.; Nowotny, J.; Gunther, W.; Klemm, E. *Macromolecules* **2003**, *36*, 5459.
- (28) Liu, M. S.; Jiang, X.; Liu, S.; Herguth, P.; Jen, A. K.-Y. *Macromolecules* **2002**, *35*, 3532.
- (29) Jayakannan, M.; Van Hal, P. J.; Janssen, R. A. J. *J. Polym. Sci. Part A: Polym. Chem.* **2002**, *40*, 251.
- (30) Jayakannan, M.; Van Hal, P. J.; Janssen, R. A. J. *J. Polym. Sci. Part A: Polym. Chem.* **2002**, *40*, 2360.

MA035576Y